	$O(8,16)^3$	$Na(11.23)^{\frac{3}{2}}$	$Si(14,28)^2$	$Ge(32,73)^{\frac{9}{2}}$	$I(53,127)^{\frac{5}{2}}$	$Xe(54,131)^{\frac{3}{2}}$	$Cs(55,133)^{\frac{7}{2}}$	$W(74,183)^{\frac{1}{2}}$
μ/μ_N	1.66812	2.21752	1.1218	−0.879467	2.81327	0.692	2.58	0.117785
F_2	4.83	13.36	4.02	−36.32	94.56	6.52	83.93	−26.30

TABLE I: Magnetic moments μ of several target nuclei used in cryogenic detectors. Here, μ_N is the proton Bohr magneton $\mu_N = e/2m_p$. The nuclear spin is denoted as superscripts. F_2 is the half of the conventional definition, $F_2 = \frac{1}{2}F_2^{\rm st}$, which is related to the effective anomalous magnetic moment corresponding to the equivalent particle that has the same mass, charge and magnetic dipole moment as the target nucleus.

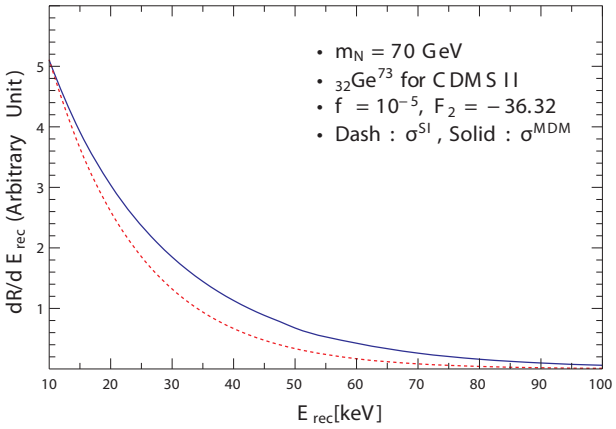

FIG. 4: WIMP(N)–nucleus detection rate as a function of the recoil energy, normalized at $E_{\rm rec} = 10$ keV. The solid line corresponds to the magnetic moment and the dashed line corresponds to the SI interaction. The MDM graph and the SI graph meet at two points due to our normalization to their equality at 10 keV. So, at very low Q^2, the MDM is bigger than SI as expected.

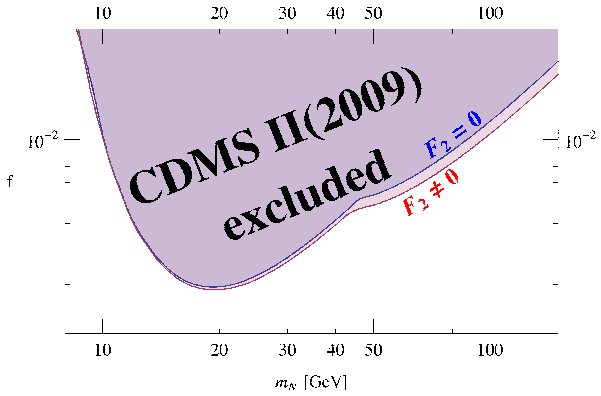

FIG. 5: The allowed region of the DM magnetic moment f vs. the DM mass m_N. The upper colored regions are excluded for $F_2 = 0$ and $F_2 \neq 0$, respectively, with the 90 % confidence level for the CDMS II data [6].

such a divergent effect is diminished by small velocity of WIMP, $v^2 \sim 10^{-6}$ which appears in the coefficient of the $1/E_{\rm rec}$-term as follows:

$$\frac{\Lambda_-}{2ME_{\rm rec}} = \frac{2M|\vec{p}|^2}{E_{\rm rec}} \simeq 2M^3\frac{v^2}{E_{\rm rec}} \simeq 2M^3\frac{10^{-6}}{10^{(-5\sim-4)}(\,{\rm GeV})}. \quad (12)$$

Due to the suppression of the IR divergent feature in non-relativistic scattering, the $dR^{MDM}/dE_{\rm rec}$ divergently larger than $dR^{SI}/dE_{\rm rec}$ only in the region below $E_{\rm rec} \sim 10\,{\rm keV}$, while the slope of the $dR^{MDM}/dE_{\rm rec}$ above $E_{\rm rec} \sim 10\,{\rm keV}$ becomes eventually more flatter than the SI. This is why the $dR^{MDM}/dE_{\rm rec}$ distribution looks larger than $dR^{SI}/dE_{\rm rec}$ above $E_{\rm rec}$ 10 keV in Fig. (4). This non-relativistic v^2- suppression in the $1/E_{\rm rec}$-term might result in further interesting possibility. Due to the suppression, 'Z terms' can be comparable to each other, even with 'F_2 terms'. In this regard, we obtain the upper-bound on the DM magnetic moment from the recent CDMS II data for both of the $F_2 = 0$ and $F_2 \neq 0$ cases. The "maximal gap method"[16] is used to estimate the proper allowed region with a 90% confidence level. The most stringent bound appears as $f \lesssim 2.88 \times 10^{-3}$ for $m_N \simeq 21$ GeV and $F_2 \neq 0$. When we ignore the contributions of nucleus anomalous magnetic moment, $F_2 = 0$, then the upper-bound of f is 1.16×10^{-2} for $m_N \sim 100\,{\rm GeV}$. Taking into account the non-zero F_2, the upper-bound goes down to 1.04×10^{-2} for $m_N \sim 100\,{\rm GeV}$. The event rate becomes larger with non-zero F_2 so that the allowed region is more constrained, producing $1 - 10\%$ of difference in f. However, we can easily expect that depending on the materials in direct detection experiments, the difference can be significantly amplified due to the enhanced magnetic dipole moment effect. Thus, it is worthwhile to study the DM multi-pole interactions with nuclei more carefully.

V. CONCLUSION

We considered a Dirac or an almost-Dirac DM N which may acquire a large magnetic moment. Using the possible dipole interactions, we estimated the signal event rate which is expected in the CDMS II experiment. Using the recent report of the CDMS II experiment, we present the upper-bound of the magnetic dipole moment. The most stringent bound appears for $m_N \simeq 21$ GeV and $F_2 \neq 0$: $f \lesssim 1.4 \times 10^{-3}$ with a sizable nucleus anomalous